

## PROPOSAL

Measurement of the neutron capture cross sections of  $^{232}\text{Th}$ ,  $^{231}\text{Pa}$ ,  $^{234}\text{U}$  and  $^{236}\text{U}$ *The nTOF Collaboration\**

Spokesperson for the nTOF Collaboration: P. Pavlopoulos

Spokesperson for this experiment: F. Gunsing

Technical Coordinator: P. Cennini

---

**Abstract**

Precise measurements of the neutron capture cross sections of nuclei relevant for the thorium-based nuclear fuel cycle are of great interest for applied physics. Specifically, a more detailed knowledge of the  $(n,\gamma)$  cross section for the isotopes  $^{232}\text{Th}$ ,  $^{231}\text{Pa}$ ,  $^{234}\text{U}$  and  $^{236}\text{U}$  is required for the possible implementation of the thorium fuel cycle in existing and innovative nuclear power devices. From a fundamental physics point of view precise measurements of the  $^{232}\text{Th}(n,\gamma)$  cross section are desirable for the study of parity non-conserving (PNC) effects in nuclei. In particular they would lead to a refined description of low-energy resonances and would allow an improved estimation of the mean value of PNC matrix elements. The high radioactivity stemming from the decay products of these isotopes has very much hindered or made impossible accurate capture measurements in the past. A significantly better situation is given at the CERN-nTOF facility which has a very favorable duty cycle for measurements on radioactive targets. We would like to make use of this advantage and propose the measurement of the cross sections of  $^{232}\text{Th}(n,\gamma)$ ,  $^{231}\text{Pa}(n,\gamma)$ ,  $^{234}\text{U}(n,\gamma)$  and  $^{236}\text{U}(n,\gamma)$  at the CERN-nTOF facility.

The proposed experiment is part of the scientific programme of the contract FIKW-CT-2000-00107 between the European Commission and the participating institutes.

U. ABBONDANNO<sup>20</sup>, G. AERTS<sup>10</sup>, S. ANDRIAMONJE<sup>10</sup>, J. ANDRZEJEWSKI<sup>24</sup>, A. ANGELOPOULOS<sup>12</sup>, P. ASSIMAKOPOULOS<sup>15</sup>, C-O. BACRI<sup>8</sup>, G. BADUREK<sup>1</sup>, E. BERTHOUMIEUX<sup>10</sup>, P. BAUMANN<sup>9</sup>, H. BEER<sup>11</sup>, J. BENLLIURE<sup>32</sup>, B. BERTHIER<sup>8</sup>, I. BONDARENKO<sup>26</sup>, C. BORCEA<sup>5</sup>, A. J. J. BOS<sup>36</sup>, E. BOSCOLO-MARCHI<sup>19</sup>, N. BUSTREO<sup>19</sup>, F. CALVINO<sup>33</sup>, D. CANO-OTT<sup>28</sup>, R. CAPOTE<sup>31</sup>, P. CARLSON<sup>34</sup>, G. CHARPAK<sup>5</sup>, N. CHAUVIN<sup>8</sup>, P. CENNINI<sup>4</sup>, V. CHEPEL<sup>25</sup>, N. COLONNA<sup>20</sup>, G. CORTES<sup>33</sup>, D. CORTINA<sup>32</sup>, F. CORVI<sup>23</sup>, A. CUSMANO<sup>21</sup>, M. DAHLFORS<sup>5</sup>, D. DAMIANOGLOU<sup>16</sup>, S. DAVID<sup>8</sup>, E. DIMOVASIL<sup>12</sup>, C. DOMINGO<sup>29</sup>, A. DOROSHENKO<sup>27</sup>, I. DURAN-ESCRIBANO<sup>32</sup>, C. ELEFThERiADIS<sup>16</sup>, M. EMBID<sup>28</sup>, L. FERRANT<sup>8</sup>, A. FERRARI<sup>5</sup>, R. FERREIRA-MARQUES<sup>25</sup>, H. FRAIS-KOELBL<sup>3</sup>, W. FURMAN<sup>26</sup>, B. FURSOV<sup>27</sup>, J. A. GARZON<sup>32</sup>, I. GIOMATARIS<sup>10</sup>, Y. GLEDENOV<sup>26</sup>, I. F. GONÇALVES<sup>40</sup>, E. GONZALEZ-ROMERO<sup>28</sup>, A. GOVERDOVSKI<sup>27</sup>, F. GRAMEGNA<sup>19</sup>, E. GRIESMAYER<sup>3</sup>, F. GUNNING<sup>10</sup>, R. HAIGHT<sup>10</sup>, M. HEIL<sup>11</sup>, A. HERRERA-MARTINEZ<sup>5</sup>, P. HOLLANDER<sup>36</sup>, K. G. IOANNIDES<sup>15</sup>, P. IOANNOU<sup>12</sup>, S. ISAEV<sup>27</sup>, E. JERICH<sup>1</sup>, Y. KADI<sup>5</sup>, F. KAEPPELER<sup>11</sup>, D. KARADIMOS<sup>17</sup>, D. KARAMANIS<sup>15</sup>, A. KAYUKOV<sup>26</sup>, L. KAZAKOV<sup>27</sup>, V. KETLEROV<sup>27</sup>, G. KITIS<sup>16</sup>, P. E. KOEHLER<sup>38</sup>, Y. KOPACH<sup>26</sup>, E. KOSSIONIDES<sup>14</sup>, I. KROSHKINA<sup>27</sup>, V. LACOSTE<sup>5</sup>, C. LAMBOUDIS<sup>16</sup>, H. LEEB<sup>1</sup>, A. LEPRETRE<sup>10</sup>, M. LOPES<sup>25</sup>, M. LOZANO<sup>31</sup>, S. LUKIC<sup>9</sup>, S. MARRONE<sup>20</sup>, J. M. MARTINEZ-VAL<sup>30</sup>, P. MASTINU<sup>19</sup>, A. MENGONI<sup>18</sup>, R. MEUNIER<sup>7</sup>, J. MEZENTSEVA<sup>26</sup>, P. MILAZZO<sup>21</sup>, E. MINGUEZ<sup>30</sup>, V. MITROFANOV<sup>27</sup>, C. MOREAU<sup>8</sup>, N. NICOLIS<sup>15</sup>, V. NIKOLENKO<sup>26</sup>, H. OBERHUMMER<sup>1</sup>, A. PAKOU<sup>15</sup>, J. PANCIN<sup>6</sup>, K. PAPADOPOULOS<sup>13</sup>, T. PAPAEVANGELOU<sup>16</sup>, C. PARADELA<sup>32</sup>, T. PARADELIS<sup>14</sup>, A. PAVLIK<sup>2</sup>, P. PAVLOPOULOS<sup>15,35</sup>, A. PEREZ-PARRA<sup>28</sup>, L. PERRIALE<sup>19</sup>, L. PERROT<sup>10</sup>, J. M. PERLADO<sup>30</sup>, V. PESKOV<sup>34</sup>, V. PIKSAIKIN<sup>27</sup>, R. PLAG<sup>11</sup>, A. PLOMPEN<sup>23</sup>, A. PLUKIS<sup>10</sup>, A. POCH<sup>33</sup>, A. POLICARPO<sup>25</sup>, A. POPOV<sup>26</sup>, Y. P. POPOV<sup>26</sup>, C. PRETEL<sup>33</sup>, J. M. QUESADA<sup>31</sup>, E. RADERMACHER<sup>4</sup>, T. RAUSCHER<sup>35</sup>, R. REIFARTH<sup>11</sup>, F. REJMUND<sup>8</sup>, C. RUBBIA<sup>22</sup>, G. RUDOLF<sup>9</sup>, P. RULLHUSEN<sup>23</sup>, L. SAKELLIU<sup>12</sup>, F. SALDANA<sup>5</sup>, J. SALGADO<sup>40</sup>, B. SAMYLIN<sup>27</sup>, I. SAVVIDIS<sup>16</sup>, S. SAVVIDIS<sup>17</sup>, P. SEDYSHEV<sup>26</sup>, J. C. SOARES<sup>40</sup>, C. STEPHAN<sup>8</sup>, P. SZALANSKI<sup>24</sup>, G. TAGLIENTE<sup>20</sup>, J. L. TAIN<sup>29</sup>, C. TAPIA<sup>33</sup>, L. TASSAN-GOT<sup>8</sup>, L. TÁVORA<sup>40</sup>, R. TERCHYCHNYI<sup>27</sup>, C. TSABARIS<sup>13</sup>, N. TSANGAS<sup>17</sup>, C. W. E. VAN EIJK<sup>36</sup>, G. VANNINI<sup>20</sup>, P. VAZ<sup>40</sup>, A. VENTURA<sup>18</sup>, A. VILLAMARIN<sup>28</sup>, V. VLACHOUDIS<sup>5</sup>, R. E. VLASTOU<sup>13</sup>, A. VOINOV<sup>26</sup>, F. VOSS<sup>11</sup>, H. WENDLER<sup>4</sup>, M. WIESCHER<sup>39</sup>, K. WISSHAK<sup>11</sup>, L. ZANINI<sup>4</sup>, S. ZEINALOV<sup>27</sup>, B. ZHURAVLEV<sup>27</sup>

1. Atominstytut der Österreichischen Universitäten, Technische Universität Wien, Austria
2. Institut für Isotopenforschung und Kernphysik, Universität Wien, Austria
3. Fachhochschule Wiener Neustadt, Wien, Austria
4. CERN, EP Division, Geneva, Switzerland
5. CERN, SL Division, Geneva, Switzerland
6. Centre National de la Recherche Scientifique/IN2P3, CENBG, Bordeaux, France
7. Centre National de la Recherche Scientifique/IN2P3, CSNSM, Orsay, France
8. Centre National de la Recherche Scientifique/IN2P3, IPN, Orsay, France
9. Centre National de la Recherche Scientifique/IN2P3, IreS, Strasbourg, France
10. Commissariat à l'Energie Atomique/DSM, Gif-sur-Yvette, France
11. Forschungszentrum Karlsruhe GmbH (FZK), Institut für Kernphysik, Germany
12. Astro-Particle Consortium, Nuclear Physics Lab., University of Athens, Greece
13. Astro-Particle Consortium, Nuclear Physics Dep., Technical University of Athens, Greece
14. Astro-Particle Consortium, Nuclear Physics Institute, NCSR "Demokritos", Athens, Greece
15. Astro-Particle Consortium, Nuclear Physics Lab., University of Ioannina, Greece
16. Astro-Particle Consortium, Nuclear Physics Lab., University of Thessaloniki, Greece
17. Astro-Particle Consortium, Nuclear Physics Dep., University of Thrace, Greece
18. ENEA, Applied Physics Division, Bologna, Italy
19. Laboratori Nazionali di Legnaro, Italy
20. Istituto Nazionale di Fisica Nuclear-Bari, Italy
21. Istituto Nazionale di Fisica Nuclear-Trieste, Italy
22. Università degli Studi Pavia, Pavia, Italy
23. JRC-EC, IRMM, Geel, Belgium
24. University of Lodz, Lodz, Poland
25. Laboratório de Instrumentação e Física Experimental de Partículas, LIP-Coimbra & Departamento de Física da Universidade de Coimbra, Portugal
26. Joint Institute for Nuclear Research, Frank Laboratory of Neutron Physics, Dubna, Russia
27. Institute of Physics and Power Engineering, Kaluga region, Obninsk, Russia
28. Centro de Investigaciones Energéticas Medioambientales y Tecnológicas, Madrid, Spain
29. Consejo Superior de Investigaciones Científicas, University of Valencia, Spain
30. Universidad Politécnica de Madrid, Spain
31. Universidad de Sevilla, Spain
32. Universidade de Santiago de Compostela, Spain
33. Universitat Politècnica de Catalunya, Barcelona, Spain
34. Kungliga Tekniska Hogskolan, Physics Department, Stockholm, Sweden
35. Department of Physics and Astronomy, University of Basel, Basel, Switzerland
36. Delft University of Technology, Interfaculty Reactor Institute, Delft, The Netherlands
37. Los Alamos National Laboratory, New Mexico, USA
38. Oak Ridge National Laboratory, Physics Division, Oak Ridge, USA
39. University of Notre Dame, Notre Dame, USA
40. Instituto Tecnológico e Nuclear - ITN

# 1 Introduction

The recent renewed interest in the nuclear fuel cycle based on  $^{232}\text{Th}$ - $^{233}\text{U}$  has made clear that the existing knowledge of reaction cross sections for many of the relevant isotopes is still rather poor. At present existing data are insufficient or lacking and severe discrepancies between the cross sections from the main neutron data libraries [1–3] exist, reflecting the fact that the evaluated files are based on only a few data sets.

A summary of the status and needs of neutron induced cross sections related to the thorium fuel cycle [4,5] indicates discrepancies up to 40% in the experimental and up to 30% in the evaluated capture data.

These uncertainties are too high for an efficiently optimized design which could simultaneously guarantee the safe operation of a thorium-cycle based accelerator driven system (ADS) and reach the design power and criticality level. The required overdimensioning will severely penalize the design and will limit the gain in flexibility in operation and design provided by the ADS subcriticality.

As an example in a specific case of a hybrid system with proton injection of constant intensity, a 10% uncertainty on the average capture cross section of  $^{232}\text{Th}$  induces a 30% uncertainty on the required proton current to have the system operating at the level of  $k_{\text{eff}} \approx 0.97$  [6].

The evaluations for the capture cross section of the isotope  $^{232}\text{Th}$  are mainly based on experiments from refs. [7–15]. For the isotopes  $^{231}\text{Pa}$ ,  $^{234}\text{U}$  and  $^{236}\text{U}$  data are more scarce and capture data are just absent or not publicly available in most cases. Evaluated cross sections are in this case based on resonance parameters from total and fission cross section measurements, published or from a compilation [16,17], and on optical model calculations in the unresolved resonance energy range.

For  $^{231}\text{Pa}$ , resonance parameters have been extracted from a total cross section measurement up to 120 eV [18] and fission has been reported from 140 to 400 keV [19]. For  $^{234}\text{U}$  fission and total cross sections from a few eV up to 8.9 MeV have been published [20]. Slightly more literature is available for  $^{236}\text{U}$ : a capture experiment from 0.01 eV up to 20 keV [21], fission between 5 and 400 eV [22], and between 5 eV and 10 keV [23], the total cross section between 40 eV and 4.1 keV [24] and the absorption between 20 eV and 1 MeV [25].

For  $^{232}\text{Th}$  the situation is different. Triggered by the increased interest in the thorium fuel cycle, several neutron capture experiments on  $^{232}\text{Th}$  have been performed recently. Most of them have been performed using the neutron time-of-flight technique. Baek *et al.* [26] investigated the gamma-ray multiplicity and the capture cross section in the energy region between 21.5 and 215 eV. Grigoriev *et al.* [27] give the average cross section in the energy region between 10 eV and 10 keV. In the unresolved resonance region, Lobo *et al.* [28] have measured the cross section between 5 and 150 keV. The measurement of Wisshak *et al.* [29] covers the region between 5 and 225 keV. Finally Karamanis *et al.* [30] use the activation technique to measure the capture cross section between 60 keV and 2 MeV. Although considerable improvement could be achieved, the discrepancies in the  $^{232}\text{Th}(n,\gamma)$  cross section below the fission threshold, i.e. in the important energy range below 1 MeV, persist.

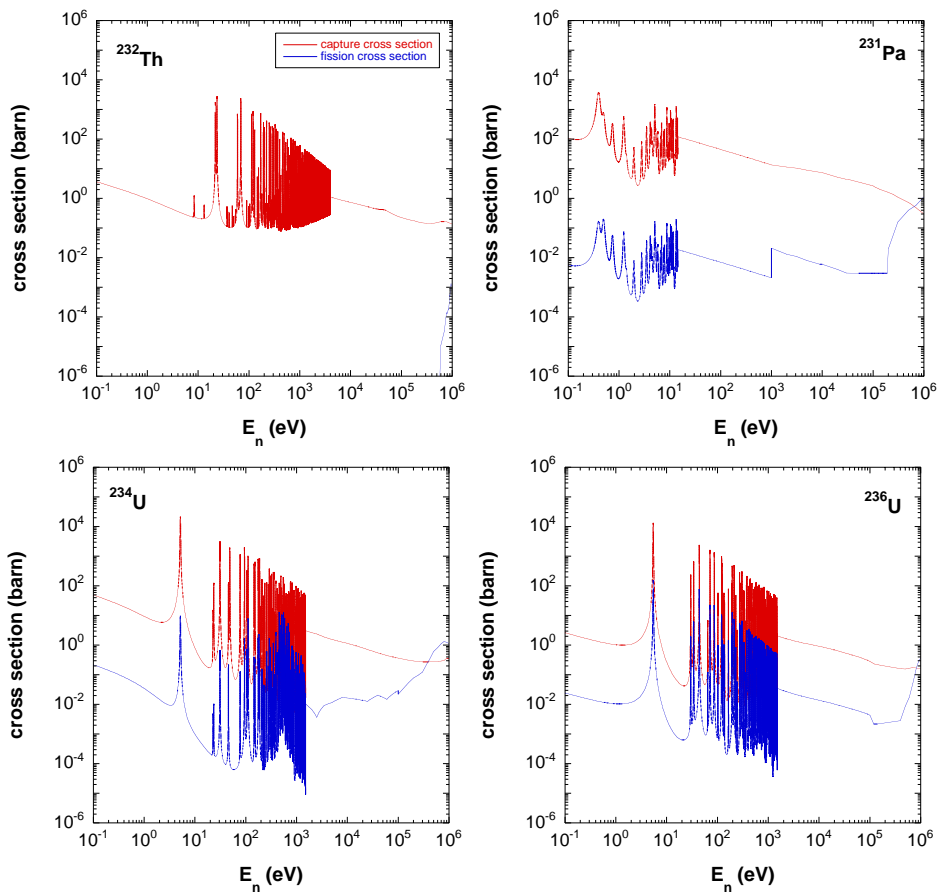


Figure 1: Evaluated neutron capture and fission cross section, Doppler broadened at 300 K, of  $^{232}\text{Th}$ ,  $^{231}\text{Pa}$ ,  $^{234}\text{U}$  and  $^{236}\text{U}$  from ENDF/B-VI [3].

The lack of capture experiments on the isotopes  $^{231}\text{Pa}$ ,  $^{234}\text{U}$  and  $^{236}\text{U}$  is related to the difficulty in obtaining suitable samples. Only  $^{232}\text{Th}$  can be obtained easily. In addition the high gamma-ray background stemming from the decay products, notably for  $^{232}\text{Th}$  and  $^{231}\text{Pa}$ , makes capture experiments rather complicated. The unique features of the CERN-nTOF facility, and especially the high instantaneous flux, allow to reduce the uncertainties due to the background radiation. In addition, the very wide energy region accessible by the facility makes it possible to cover the energy region of interest from 1 eV up to 1 MeV in a single experiment.

In figure 1 the capture cross sections for  $^{232}\text{Th}$ ,  $^{231}\text{Pa}$ ,  $^{234}\text{U}$  and  $^{236}\text{U}$  are shown. For comparison also the fission cross section is given. The subthreshold fission cross section for  $^{232}\text{Th}$  is absent and is about two orders of magnitude lower for  $^{231}\text{Pa}$ ,  $^{234}\text{U}$  and  $^{236}\text{U}$  in most of the energy range of interest. The measurement of the  $^{232}\text{Th}(n,\gamma)$ ,  $^{231}\text{Pa}(n,\gamma)$ ,  $^{234}\text{U}(n,\gamma)$  and  $^{236}\text{U}(n,\gamma)$  neutron capture cross section is part of the scientific programme of the contract FIKW-CT-2000-00107 between the European Commission and the participating institutes. Nuclear data needs for isotopes for the thorium cycle are expressed in Work Package 12 of this contract listing the capture cross sections to be delivered, namely that of the isotopes  $^{232}\text{Th}$ ,  $^{231}\text{Pa}$ ,  $^{233}\text{U}$ ,  $^{234}\text{U}$  and  $^{236}\text{U}$ . For  $^{232}\text{Th}$  a ready-to-use sample is available and the handling of the target material is possible within the current safety regulations. For the three isotopes  $^{231}\text{Pa}$ ,  $^{234}\text{U}$  and  $^{236}\text{U}$  the availability of sufficient material in the form of a suitable sample is being investigated.

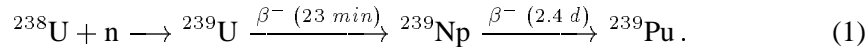
We present them in the context of this proposal, giving count rate estimations adaptable to the finally available samples. The fissile isotope  $^{233}\text{U}$  cannot be measured with the presently available  $\text{C}_6\text{D}_6$  detectors. A proposal for this isotope will be submitted later for an experiment with the planned  $4\pi$  calorimeter.

In the unresolved resonance region the cross sections are in general rather smooth and can be well presented in tabular form. At lower energies one can resolve individual resonances. The measured resonances are broadened by the Doppler effect and the finite resolution of the spectrometer. Therefore one usually describes the cross section in this energy region with resonance parameters using the  $R$ -matrix formalism, which are independent from the experimental setup. The resonance parameters represent the properties of the excited states of the compound nucleus, like the energy, spin, parity and the partial widths. In this way, the resonance parameters allow to reconstruct the cross sections (not only the capture cross section) for any application.

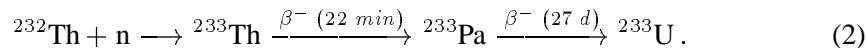
We propose to measure at the CERN-nTOF facility the capture cross sections of  $^{232}\text{Th}$ ,  $^{231}\text{Pa}$ ,  $^{234}\text{U}$  and  $^{236}\text{U}$  in the resolved resonance energy region as well as at higher energies up to close to the fission threshold and below 1 MeV with an accuracy better than 5%. The data in the resolved resonance region will be analyzed in terms of resonance parameters taking into account the specific conditions of the experimental setup. In addition, information on the level density of highly excited nuclei, an important ingredient in many nuclear models, is obtained directly from resolved resonances, and will be addressed by the high energy resolution of the CERN-nTOF facility at low neutron energies. Although we must put in the analysis emphasis on the nuclear data aspects of these measurements, we will also consider the implications of our data for  $^{232}\text{Th}$  on the estimation of the PNC matrix elements.

## 2 The thorium fuel cycle

Conventional nuclear power reactors are based on the fission process of  $^{235}\text{U}$  and  $^{239}\text{Pu}$ . While  $^{235}\text{U}$  is fissile, the fertile uranium isotope  $^{238}\text{U}$ , which is largely present in the fuel (97%), becomes the fissile  $^{239}\text{Pu}$  during the use of the fuel due to neutron capture followed by  $\beta$ -decay



An alternative fuel cycle is based on the use of thorium in nuclear reactors. In this cycle  $^{233}\text{U}$  is the fissile isotope which is formed from  $^{232}\text{Th}$  by neutron capture followed by  $\beta$ -decay



A very interesting advantage from the point of view of production of radioactive waste in using the  $^{232}\text{Th}/^{233}\text{U}$ -based fuel cycle as compared to the classic uranium cycle is related to its low production in of higher mass actinides. The lower atomic number of

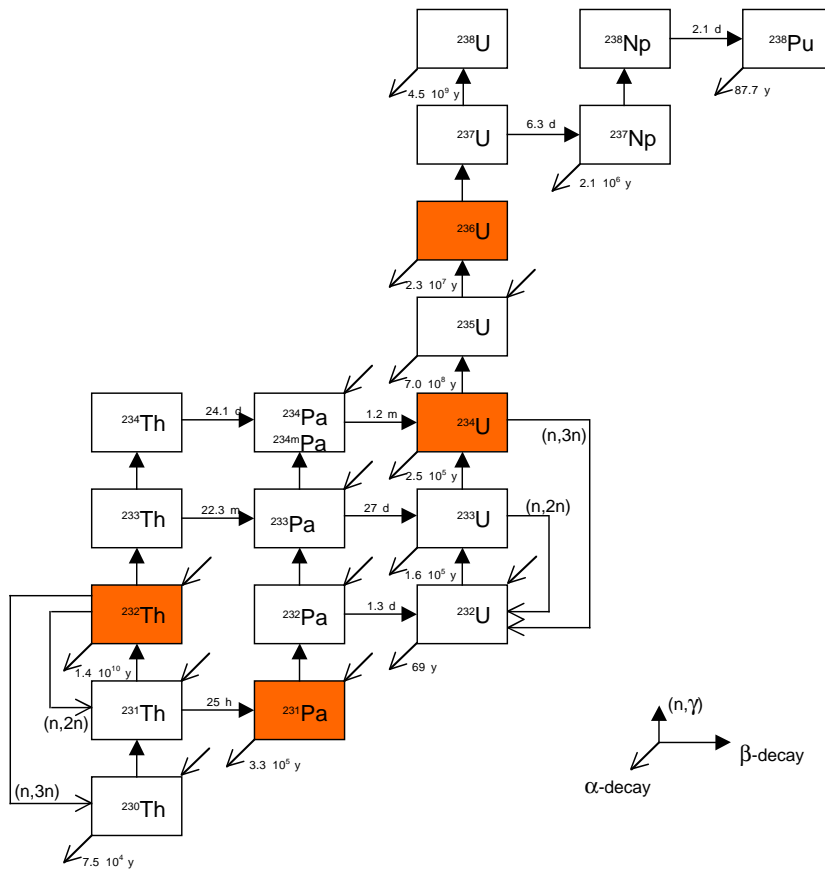


Figure 2: Schematic view of the isotope formation in the thorium cycle. The in this paper proposed isotopes are presented in a shaded box.

thorium ( $Z = 90$ , instead of  $Z = 92$  for uranium) reduces significantly the build-up of heavy transuranium isotopes, in particular plutonium and curium. This is also clearly demonstrated by detailed simulations on the isotopic composition of a thorium-based ADS system [31]. In figure 2 a schematic view of the isotope formation in the thorium cycle is shown.

In addition other arguments, although less important in the present context, play a role. The natural abundance of thorium is three times larger than that of uranium so extends potentially the existing fuel resources. Also the number of neutrons produced after absorption of a neutron in a reactor environment is larger for  $^{233}\text{U}$  than for  $^{235}\text{U}$  or  $^{239}\text{Pu}$  for thermal neutrons, opening the possibility, although technically still quite complicated, for a “thermal breeder”.

Several experimental projects using thorium have already been worked out in critical assemblies (Molten Salt Reactor, CANDU-Th, High-Temperature Gas Reactor). Due to encountered technical problems but also overshadowed by the rapid industrialized production of uranium-based reactors, most of the research and development has been focussed on the uranium based cycle and is at present missing for thorium. In fact all operating power plants are working with a uranium-based fuel cycle today.

The growing concern of the public opinion on nuclear waste and inherently safely operating nuclear energy systems has led to a variety of research activities. The use

of thorium in the nuclear fuel cycle for either critical or subcritical systems is nowadays a topic of interest.

Recently, many developments and studies have been devoted to subcritical reactors driven by an accelerator. Such an ADS has clear advantages on the criticality and safety aspects of nuclear energy production as compared to critical assemblies and opens new perspectives for nuclear waste management [32,33]. This type of reactors can be used to incinerate radioactive waste (primarily long-lived minor actinides), to burn the massive stocks of plutonium, or to produce energy in an efficient and safe way. An innovative concept using an ADS with  $^{232}\text{Th}/^{233}\text{U}$  is the Energy Amplifier [34].

The present state of the description of the thorium-cycle related cross sections is not yet at the level of that of the uranium cycle. The conceptualization and realization of nuclear power stations based on the use of thorium, either in a critical or subcritical system, require a good knowledge of the reaction cross sections of the thorium cycle isotopes. As indicated in "The NEA high priority nuclear data request list" [35], the capture cross section of  $^{232}\text{Th}$  with uncertainties smaller than 5% are needed in the region between 1 eV and 500 keV. A precision of even 1-2% for  $^{232}\text{Th}$  and somewhat less stringent up to 5-10% for  $^{231}\text{Pa}$ ,  $^{234}\text{U}$  and  $^{236}\text{U}$  is requested in a dedicated study on nuclear data needs for the thorium fuel cycle [4,5].

### 3 Resonance parameters of $^{232}\text{Th}$ for parity violation

The relative strength of the weak parity nonconserving part (PNC) part of the nucleon-nucleon force as compared with the strong parity conserving (PC) interaction is about  $10^{-7}$ . A significant enhancement of the PNC part may occur in highly excited compound nuclei due to the mixing of nuclear levels of the same (channel) spin and opposite parity [36,37]. In heavy nuclei the combination of kinematic and dynamical enhancements may amplify the PNC effects by  $10^4$  to  $10^6$ . Such enhanced PNC effects in  $p$ -wave resonances have been measured first in Dubna [38] and were followed by a large series of transmission measurements in Los Alamos with low-energy polarized neutrons using different nuclei for the unpolarized target. In these measurements, which include also  $^{232}\text{Th}$  [39–41], PNC-effects as large as 10% have been observed.

PNC-effects are particularly prominent in  $p$ -wave resonances and can be explained by the admixing of nearby  $s$ -wave resonances with the same channel spin. The  $p$ -wave resonance cross section  $\sigma_p^\pm$  for neutrons with positive, respectively negative helicity is related to the parity violating asymmetry  $P$  by  $\sigma_p^\pm = \sigma_p(1 \pm P)$ , which can be described for a spin zero target nucleus in a two-level approximation by

$$P = \frac{2V_{sp}}{E_s - E_p} \frac{\sqrt{\Gamma_n^s}}{\sqrt{\Gamma_n^p}}, \quad (3)$$

where  $V_{sp}$  is the PNC matrix element between  $s$ - and  $p$ -wave states and where  $\Gamma_n^s$  and  $\Gamma_n^p$  are the neutron decay widths for  $s$ - and  $p$ -wave resonances respectively. The small difference in energy of the two levels and the large difference in their neutron entrance channel widths, for  $p$ -waves typically a factor  $10^3$  smaller than for  $s$ -waves in this mass and energy region, have as a consequence that PNC effects are largest in low-energy neutron  $p$ -wave resonances of heavy and medium mass nuclei.

The matrix elements  $V_{sp}$  for the  $p$ -wave resonances, derived from the measured asymme-

tries and known resonance neutron widths and energies, are supposed to have a Gaussian distribution with zero mean and variance  $M^2$ . For the ensemble of  $p$ -wave resonances one can via statistical analysis estimate the root mean squared value of the PNC matrix element  $\sqrt{M^2}$  in nuclear matter, revealing the overall strength of the weak interaction in the nucleus.

PNC has been observed in neutron resonances of several target nuclei in the successful TRIPLE experiments at Los Alamos. In general the deduced  $M$ -values are qualitatively consistent with the theoretical expectation. The case of  $^{232}\text{Th}$  is an exception because the signs of the asymmetries of almost all resonances are positive. This deviation from the general picture suggests that the sign correlation observed in  $^{232}\text{Th}$  is specific, and is not a general feature of the weak nucleon-nucleus interaction. A large number of possible theoretical explanations for this sign correlation have been worked out but so far none of them are really satisfactory.

The asymmetries of the  $p$ -wave resonances in  $^{232}\text{Th}$  have been measured up to 300 eV at Los Alamos. The better resolution of the nTOF facility opens the possibility in future to study PNC effects at even higher resonance energies, provided that a neutron polarizer is installed.

The resonance energies are rather well known. However, due to the small cross sections of low-energy  $p$ -wave resonances, very little attention has been paid to them since, apart from the information they contain concerning the level density, they do not contribute significantly to multigroup cross sections. A more precise knowledge of the  $p$ -wave neutron widths  $\Gamma_n$  may improve the extraction of the matrix elements  $V_{sp}$  from the measured asymmetries  $P$  and in this way ameliorate the interpretation of these data.

## 4 Experimental setup

The neutron capture experiments will be performed using  $\text{C}_6\text{D}_6$  gamma-ray detectors together with a pulse height weighting technique [42–44]. Pulse height weighting is a method of making the detection efficiency independent of the gamma-ray cascade of the  $(n,\gamma)$  reaction and is based on low-efficiency detectors in order to detect not more than a single gamma ray per cascade.

We plan to use  $\text{C}_6\text{D}_6$ -based gamma-ray detectors in a standard 90 degrees geometry. The overall detection efficiency for a capture event, taking into account the gamma-ray multiplicity, is about 20% in this configuration. A schematic view of the setup is shown in figure 3.

The liquid scintillator detectors based on deuterated benzene  $\text{C}_6\text{D}_6$  have an overall efficiency (including solid angle) of a few percent for gamma rays in the range of interest between 0.1-10 MeV. They have also the advantage of being the least sensitive to scattered neutrons as compared to other gamma-ray detectors. However, it is not possible with  $\text{C}_6\text{D}_6$ -based detectors in the standard setup to distinguish whether the detected gamma rays originate from the  $(n,\gamma)$  reaction, the radioactive background or from competing reaction channels like fission or inelastic scattering.

The quantity determined in a neutron capture experiment is the capture yield, i.e. the fraction of neutrons incident on a sample (with thickness  $n$  atoms per barn) and



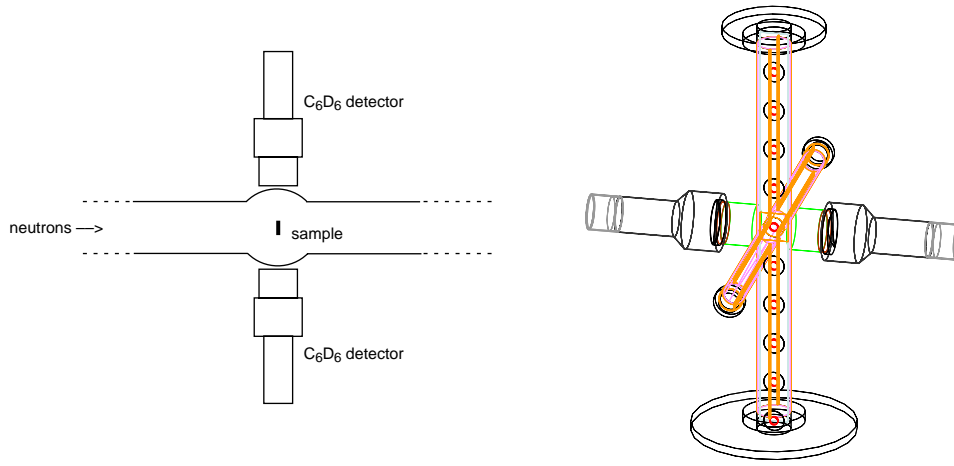


Figure 3: Experimental setup of the capture experiment. In the left panel a schematic top view is shown. In the right panel a three dimensional visualization of the simulated geometry from [46] is presented.

undergoing the  $(n,\gamma)$  interaction. The capture yield  $Y(E)$ , with  $0 < Y(E) < 1$ , for the first interaction can be written as

$$Y(E) = \left(1 - e^{-n\sigma_T(E)}\right) \frac{\sigma_\gamma(E)}{\sigma_T(E)} \approx \begin{cases} n\sigma_\gamma & \text{if } n\sigma_T \ll 1 \\ \sigma_\gamma/\sigma_T & \text{if } n\sigma_T \gg 1 \end{cases} \quad (4)$$

with  $\sigma_T$  the total and  $\sigma_\gamma$  the neutron capture cross section. The two limiting cases are approximations for thin respectively thick samples. Since the efficiency of the capture detector and solid angle of the detector are far below 100%, the measured time-of-flight spectra need to be normalized to a well known isotope in order to extract the normalization constant, representing the solid angle and the detector efficiency. We will use the first large resonance at 4.9 eV in  $^{197}\text{Au}$  for this purpose in combination with the smooth cross section between 10 and 100 keV which is a standard.

Simultaneously with the capture spectrum, the shape of the neutron flux is recorded by means of a monitoring system based on silicon detectors. The combination of the capture spectrum and the flux spectrum allows to determine the capture yield to be used in further analysis.

## 5 Sample availability and safety aspects

A  $^{232}\text{Th}$  sample of 1.77 g from IRMM-Geel and presently located at FZK-Karlsruhe where it has been measured [29], will be used for the  $^{232}\text{Th}$  measurements. This selfsupporting metallic sample of cylindrical shape has a diameter of 15 mm so a thickness of  $1.0 \text{ g/cm}^2$  or  $2.6 \times 10^{-3}$  atoms/barn. A specific activity of 41 kBq/g corresponds to  $^{232}\text{Th}$ .

We would like to use the  $^{232}\text{Th}$  without canning. The three other isotopes  $^{231}\text{Pa}$ ,  $^{234}\text{U}$  and  $^{236}\text{U}$  will be used as samples in sealed cannings consisting of Ti or Al.

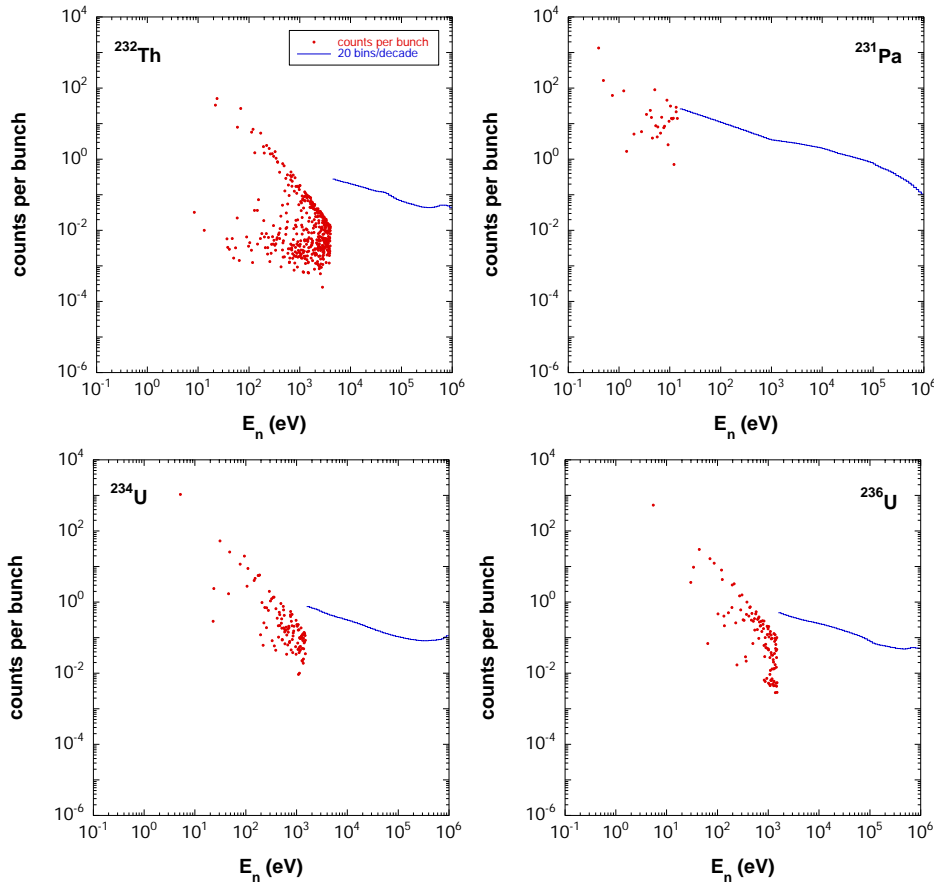


Figure 4: Estimated count rate for the presented capture setup with 20% efficiency, normalized to 1 gram of the indicated isotope.

About 1 g of  $^{231}\text{Pa}$  in the form of  $\text{Pa}_2\text{O}_5$  can be borrowed from ITU-Karlsruhe. Taking into account the present isotopical composition due to its decay products, the activity of this material is close to 80 GBq. Possibly only a fraction of this quantity can be handled even in a sealed form.

The uranium isotopes can be supplied in a chemically and isotopically purified oxide form by the participating institutes of Dubna and Obninsk. About 100 mg of  $^{234}\text{U}$  and 1 g of  $^{236}\text{U}$  are available having a specific *alpha*-activity of 240 MBq/g and 2.4 MBq/g respectively.

## 6 Count rate estimations

In order to estimate the expected count rate we have to divide the capture cross section in two parts. One part concerns the resolved resonances, where the aim is to extract the resonance parameters. Cross sections for resolved resonances are usually given in terms of resonance parameters instead of in tabulated form. For count rate estimations it is therefore more convenient to use the resonance area. An isolated resonance at low energy can be described in the single level Breit-Wigner approximation of the  $R$ -matrix

formalism as

$$\sigma_{\gamma}(E) = \pi \lambda^2 g \frac{\Gamma_n \Gamma_{\gamma}}{(E - E_0)^2 + \Gamma^2/4} \quad (5)$$

where  $\Gamma_n$  is the neutron width,  $\Gamma_{\gamma}$  is the radiative width,  $g$  the statistical spin factor and  $\lambda$  the reduced de Broglie wave length of the neutron. The integral  $I_{\sigma}$  of the resonance is then taken as

$$I_{\sigma} = 2 \int_{E_0 - \Gamma/2}^{E_0 + \Gamma/2} \sigma_{\gamma}(E) dE = 2\pi^2 \lambda^2 g \frac{\Gamma_n \Gamma_{\gamma}}{\Gamma} \quad (6)$$

In the unresolved resonance region where the cross section is smooth, a division in log-equidistant bins is appropriate. In this region, the quantity  $I_{\sigma}$  corresponds to the average cross section in the bin, multiplied by the bin width.

Approximating the yield by  $Y = n \times \sigma_{\gamma}$ , which is valid for this purpose except for a few large resonances at low energy, we can define the count rate  $C_{\gamma}(E_0)$  integrated over a resonance or over a bin centered at energy  $E_0$  as

$$C_{\gamma}(E_0) = A \times \nu_{\gamma} \times n \times I_{\sigma} \times \varphi(E_0) \times \epsilon \quad \text{counts} \cdot \text{bunch}^{-1} \quad (7)$$

where  $A$  is the surface of the sample,  $\epsilon$  the absolute efficiency (taken as 3% for a single 1 MeV gamma ray for one Bicron  $C_6D_6$  detector as calculated with the code GEANT4 [46], and independently with MCNP4C) including the solid angle,  $\nu_{\gamma}$  is the gamma-ray multiplicity, taken as 3 for the here proposed nuclei, and where  $\varphi(E_0)$  is the neutron flux for one typical proton pulse of  $7 \times 10^{12}$  protons, at the neutron energy  $E_0$ , taken constant over the resonance. Note that the total efficiency for a capture event, including the multiplicity, is nearly 20% for a 2 detector system. We have used the collimated flux at the sample position averaged over the surface of a sample with a radius of 7.5 mm, corresponding to the simulated flux at 200 m [47] divided by a factor of 2 to take into account the smaller distance at 185 m and the flux reduction due to the collimators. This flux has been fitted in the energy range between 1 eV and 1 MeV as

$$\varphi(E) = 3.9 \times 10^3 E^{-0.973} \quad \text{neutrons} \cdot \text{cm}^{-2} \cdot \text{eV}^{-1} \cdot \text{bunch}^{-1} \quad (8)$$

In figure 4 we show the expected count rates for the resolved resonances together with the unresolved resonance region given in 20 bins per decade corresponding to a bin width of roughly 10% of the neutron energy.

## 7 Background

Several sources of background will affect the measurements. Where for the resolved resonances shape analysis may partly reduce this problem, for a smooth cross section at higher incident neutron energies one need to address all components and subtract them accordingly.

The background due to radioactivity is strongly suppressed at the nTOF facility. In  $^{232}\text{Th}$  the high energy gamma rays going up to 2.6 MeV originating from the beta decay of the daughter product  $^{208}\text{Tl}$  were particularly hindering previous capture measurements. The strong reduction of this background is demonstrated in figure 5.

The effect of gamma rays induced by sample scattered neutrons is for this isotope in this energy range only a few percent at maximum and can be corrected for by a calculated

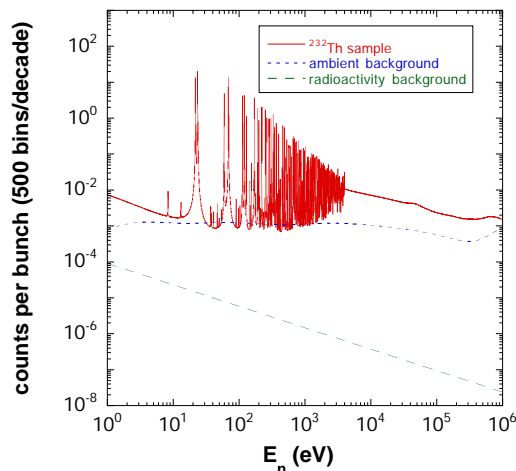


Figure 5: Estimated count rate and expected ambient and radioactive background in a single  $C_6D_6$  detector with 500 bins/decade for the 1.77 g sample of  $^{232}Th$ .

neutron sensitivity. The background from sample scattered photons might be larger. This effect will be assessed experimentally and more quantitatively, also by simulations, after the winter stop when the background shielding will be completed. The ambient background as measured in September-November 2001 [48], corresponding to no sample in the beam, is shown in figure 5 together with as an example the computed count rate of the 1.77 g sample of  $^{232}Th$  using 500 bins per decade to make the resonance shape visible.

Also inelastic neutron scattering, a reaction channel that opens at the excited states of the target nucleus, causes a gamma-ray background. The effect from inelastic scattering can be reduced by choosing appropriately higher thresholds, eliminating the low-energy gamma rays resulting from the decay of the lowly excited nucleus to the ground state. Since the nTOF data acquisition system allows to set this threshold in the analysis phase, we can apply off-line higher thresholds in the energy region above a few hundreds of keV where inelastic scattering becomes non-negligible.

Below the fission threshold prompt photons from fission do not play a role but delayed photons from fission fragments with a longer half-life may be detected at lower times of flight and contribute to the background. However, most of the fission products are beta emitters and the distribution of their half-lives is very broad. The majority of the fission products [49] have half-lives larger than the time window after the pulse where data is acquired and will therefore be seen as a constant background, which should be measured immediately after irradiation.

## 8 Beam time request

The four isotopes presented in this proposal have to be considered in the same context concerning both the measurement techniques and the physical applications. Nevertheless, the sample availability and preparation form a supplementary degree of difficulty and is at present not defined in all practical details for all isotopes. Apart from  $^{232}Th$ , for which the sample is ready to use, the final masses of the samples of  $^{231}Pa$ ,  $^{234}U$  and

Table 1: Estimation of the needed protons.

#	isotope	probable mass (g)	count rate limit (cnts/bnch/g)	stat. prec. (%)	nr. of protons ( $\times 10^{18}$ )
1	$^{232}\text{Th}$	1.77	0.03	1	1.3
2	$^{231}\text{Pa}$	0.2	0.10	2	0.9
3	$^{234}\text{U}$	0.1	0.07	2	2.5
4	$^{236}\text{U}$	1.0	0.04	2	0.5

$^{236}\text{U}$ , will be defined later. We intend to present later an additional proposal to measure part of the isotopes with the  $4\pi$  calorimeter to be constructed, gaining in this way a discrimination against fission and inelastic scattering and a factor 5 in efficiency. This holds in particular for  $^{234}\text{U}$  for which available sample mass is small and where the fission contribution becomes already at 100 keV a non-negligible background. Additional technical and status information can be supplied to the INTC in due time. The request on the number of protons is based on the count rate estimations shown in figure 4. The requested statistical uncertainty on the lower count rate limit are given in table 1 as well as the probable mass. For  $^{232}\text{Th}$ , for which the precision needs are more tight, we would like to obtain a statistical precision of 1% in the high energy region below 1 MeV with an energy resolution of 20 bins/decade, while for the other isotopes we aim at 2%. The final obtainable precision will be larger because the experimental backgrounds, which have to be measured, have to be taken into account. Although the final background that will be present has to be experimentally verified, a total uncertainty better than 5% may be expected.

In order to use the time more effectively and reduce the mission load for the participating institutes, we would like to request the possibility to use at least 4 bunches per supercycle for a large fraction of the running time corresponding to these experiments.

## References

- [1] C. Nordborg, M. Salvatores, *Status of the JEF Evaluated Data Library*, Nuclear Data for Science and Technology, edited by J. K. Dickens (American Nuclear Society, LaGrange, IL, 1994)
- [2] T. Nakagawa, et al., Japanese Evaluated Nuclear Data Library, Version 3, Revision 2, *J. Nucl. Sci. Technol.* **32** 1259 (1995)
- [3] Cross Section Evaluation Working Group, *ENDF/B-VI Summary Documentation*, Report BNL-NCS-17541 (ENDF-201) (1991), edited by P.F. Rose, National Nuclear Data Center, Brookhaven National Laboratory, Upton, NY, USA.
- [4] B. D. Kuzminov and V. N. Manokhin, in: *Proc. Int. Conf. Nuclear Data for Science and Technology*, Vol. 59 II, Eds. G. Reffo, A. Ventura and C. Grandi, Bologna (1997) 1167
- [5] V. G. Pronyaev, report INDC(NDS)-408 (1999)
- [6] M. Salvatores, in: *Proc. Int. Conf. Nuclear Data for Science and Technology*, Vol. 59 I, Eds. G. Reffo, A. Ventura and C. Grandi, Bologna (1997) 3
- [7] F. Rahn *et al.*, *Phys. Rev. C* **6** (1972) 1854
- [8] M. Lindner *et al.*, *Nucl. Sci. and Eng.* **59** (1976) 381
- [9] R. L. Macklin and J. Halperin,, *Nucl. Sci. and Eng.* **64** (1977) 849
- [10] P. Poenitz, ANL/NDM-45 (1978)
- [11] K. Kobayashi *et al.*, *J. Nucl. Sci. Techn.* **18** (1981) 823

- [12] R. L. Macklin, *Nucl. Sci. Eng.* **79** (1981) 118
- [13] D. K. Olsen, R. W. Ingle, J. L. Portney, *Nucl. Sci. Eng.* **82** (1982) 289
- [14] R. B. Perez *et al.*, *Nucl. Sci. and Eng.* **80** (1982) 189
- [15] K. Kobayashi *et al.*, *Ann. Nucl. Energy* **15**(8) (1988) 381
- [16] S. F. Mughabghab, M. Divadeenam and N. E. Holden, *Neutron Cross Sections; Neutron resonance parameters and thermal cross sections* (Academic Press, New York, 1981)
- [17] S. Sukhoruchin, Z. N. Soroko, V. V. Deriglazov, *Low Energy Neutron Physics, volume I/16B* ed. H. Schopper, (Springer, Landolt-Börnstein 1998)
- [18] A. Hussein *et al.*, *Nucl. Sci. Eng.* **78** (1981) 370
- [19] S. Plattard *et al.*, *Phys. Rev. Lett.* **46**(10) (1981) 633
- [20] G. D. James *et al.*, *Phys. Rev. C* **15**(6) (1977) 2083
- [21] A. D. Carlson *et al.*, *Nucl. Phys.* **A141** (1970) 577
- [22] J. P. Theobald *et al.*, *Nucl. Phys.* **A181** (1972) 639
- [23] W. E. Parker *et al.*, *Phys. Rev. C* **49**(2) (1994) 673
- [24] G. Carraro and A. Brusegan, *Nucl. Phys.* **A257** (1976) 333
- [25] R. L. Macklin and C. W. Alexander, *Nucl. Sci. Eng.* **104** (1990) 258
- [26] W. Y. Baek *et al.*, *Nucl. Instr. Meth.* **B168** (2000) 453
- [27] Yu. V. Grigoriev *et al.*, *Proc. Int. Sem. Interact. Neutrons with Nuclei, ISINN-8*, Dubna (2000) 68
- [28] G. Lobo *et al.*, *proc. Nucl. Data. Sci. Techn.*, Tsukuba, 2001
- [29] K. Wisshak, F. Voss, and F. Käppeler, *Nucl. Sci. and Eng.* **137** (2001) 183
- [30] D. Karamanis *et al.*, *Nucl. Sci. and Eng.* **139** (2001) 282
- [31] J. García-Sanz *et al.*, in: *Proc. Int. Conf. Acc. Driven Transm. Techn. Appl. ADTTA*, Prague (1999)
- [32] C. Rubbia *et al.*, *A realistic plutonium elminiation scheme with fast energy amplifiers and thorium-plutonium fuel*, report CERN/AT/95-53(ET), CERN (1995)
- [33] E. González *et al.*, in: *Proc. Actinide and Fission Product Partitioning and Transmutation, 6th Information Exchange Meeting*, Madrid (2000) 207
- [34] C. Rubbia *et al.*, *Conceptual design of a fast neutron operated high power energy amplifier*, report CERN/AT/95-44(ET), CERN (1995)
- [35] NEA Nuclear Science Committee, Working Party on International Evaluation Cooperation, Subgroup C, *The NEA High Priority Nuclear Data Request List*, Status in March 2001
- [36] G. E. Mitchell, J. D. Bowman and H. A. Weidenmüller, *Rev. Mod. Phys.* **71**, (1999) 445
- [37] G. E. Mitchell, J. D. Bowman, S. I. Pentillä and E. I. Sharapov, *Phys. Rep.* **354** (2001) 157
- [38] V. P. Alfimenkov *et al.*, *Nucl. Phys.* **A398** (1983) 93
- [39] C. M. Frankle *et al.*, *Phys. Rev. C* **46** (1992) 778
- [40] J. D. Bowman, G. T. Garvey and M. B. Johnson, *Annu. Rev. Nucl. Part. Sci.* **43** (1993) 829
- [41] S. L. Stephenson *et al.*, *Phys. Rev. C* **58** (1998) 1236
- [42] F. Corvi, A. Prevignano, H. Liskien and P.B. Smith, *Nucl. Instr. and Meth.* **A265** (1988) 475
- [43] F. Corvi, G. Fioni, F. Gasperini and P.B. Smith, *Nucl. Sci. and Eng.* **107** (1991) 272
- [44] J. L. Tain *et al.*, *Proc. Int. Conf. Nucl. Data for Science and Techn.*, Tsukuba, Oct. 7-12, 2001
- [45] D. Cano-Ott, E. González-Romero, M. Embid, Report CIEMAT, DFN/TR-01/II-02 (2001)
- [46] C. Domingo-Pardo, *Trabajo de Investigación*, University of València, 2001
- [47] V. Vlachoudis, private communication.
- [48] The nTOF collaboration, report CERN/INTC 2001-038 (2001)
- [49] T. R. England and B. F. Rider, Los Alamos National Laboratory report LA-UR-94-3106, ENDF-349 (1993)